ISSN 1070-3284, Russian Journal of Coordination Chemistry, 2014, Vol. 40, No. 4, pp. 205–215. © Pleiades Publishing, Ltd., 2014.
Original Russian Text © A.V. Piskunov, I.N. Meshcheryakova, G.K. Fukin, I.V. Smolyaninov, N.M. Khamaletdinova, O.V. Kuznetsova, 2014, published in Koordinatsionnaya Khimiya, 2014, Vol. 40, No. 4, pp. 205–215.

Tin(IV) Complexes Based on 2-Hydroxy-3,6-Di-*tert*-Butyl-*para*-Benzoquinone: Syntheses, Structures, and Electrochemical Behavior in Solution

A. V. Piskunov[a, *], I. N. Meshcheryakova[a], G. K. Fukin[a], I. V. Smolyaninov[b], N. M. Khamaletdinova[a], and O. V. Kuznetsova[a]

[a] *Razuvaev Institute of Organometallic Chemistry, Russian Academy of Sciences, ul. Tropinina 49, Nizhni Novgorod, 603950 Russia*

[b] *Research Group of Toxicology, Department of Aqua Culture and Water Resources, Southern Scientific Center, Russian Academy of Sciences, Astrakhan, Russia*

**e-mail: pial@iomc.ras.ru; thiophen@mail.ru*

Received July 23, 2013

Abstract—A series of new tin(IV) complexes based on 2-hydroxy-3,6-di-*tert*-butyl-*para*-benzoquinone (LH) of the general formula L_2SnR_2 (R = Me (**I**), Et (**II**), Bu^n (**III**), Ph (**IV**)) and $LSnMe_3$ (**V**) were synthesized. The obtained compounds were characterized by IR and ^1H, ^{13}C and ^{119}Sn NMR spectroscopy and elemental analysis. The X-ray diffraction analysis was carried out for complexes $L_2Sn(Bu^n)_2$ (**III**) and $LSnMe_3$ (**V**). The low-frequency region of the IR spectra, which has not earlier been studied in detail, was interpreted for compounds **I**–**V** and previously described complex $LSnPh_3$ (**VI**). The electrochemical properties of LH and related tin complexes **I**–**VI** were studied. The nature of the hydrocarbon groups at the metal atom affects the stability of the intermediates formed in the electrochemical reactions.

DOI: 10.1134/S1070328414040083

INTRODUCTION

This work continues the studies of nontransition metal complexes based on the redox-active ligands actively developed in recent decades. The development of this direction in the chemistry of coordination and organometallic compounds is urgent and promising as demonstrated by examples of an unusual reactivity of this class of compounds (in particular, in redox transformations). Among the most interesting results are the discovery of the unique ability of the antimony(V) catecholate and amidophenolate complexes to reversibly add oxygen [1–5], nitrogen monoxide fixation by the lead(II) and zinc(II) catecholate derivatives [6], the activation of the triple bond in terminal alkynes in the reactions with the aluminum(III) and gallium(III) compounds based on the acenaphthenediimine ligand [7–9], and the oxidative addition of alkyl halides to the indium(III) bis(amidophenolate) complexes [10]. The above examples concern the metal compounds containing redox-active ligands in the reduced form. However, ligands of this type can exist in the coordination sphere of metal atoms in the neutral form as well. For example, the zinc(II) and indium(III) compounds containing the coordinated *o*-benzoquinone or *o*-iminobenzoquinone molecule were described [11, 12]. These complexes act in reactions as oxidants rather than reducing agents. The oxidation ability of the redox-active ligand neutrally bound to the metal atom is noticeably enhanced compared to that of free *o*-benzoquinone (*o*-iminobenzoquinone).

This work is devoted to the synthesis and study of the physicochemical properties of the tin(IV) complexes based on the *p*-benzoquinone ligand additionally functionalized by the hydroxy group (LH). These compounds also act as oxidants in redox processes, and the study of their redox potentials and redox transformations seems to be very interesting. In addition, the study of these complexes is urgent from the viewpoint of prospects of their use as biologically active substances. It has recently been shown that the organotin compounds based on dihydroxy-9,10-anthracenedione and hydroxy-1,4-naphthoquinone [13–15] are the closest analogs of the compounds studied by us and exhibit a high anticancer activity.

EXPERIMENTAL

The reagents used were synthesized according to known procedures: LH [16], $LSnPh_3$ [16], $ClSnMe_3$, Cl_2SnMe_2, Cl_2SnEt_2, $Cl_2Sn(Bu^n)_2$ (Bu^n = *n*-butyl), and Cl_2SnPh_2 [17].

NMR spectra were detected in a $CDCl_3$ solution at 20°C on Bruker DPX-200 (200 MHz) and Bruker Avance III (400 MHz) instruments using tetramethylsilane as an internal standard.

IR absorption spectra in the medium region were recorded on an FSM 1201 FT-IR spectrometer in the spectral range from 450 to 4000 cm^{-1} with a resolution of 4 cm^{-1} (scan number 32). The samples were prepared as suspensions in Nujol between potassium bromide windows. The far-IR spectra were recorded on a Vertex 70 FT-IR spectrometer (Bruker) in the range from 600 to 150 cm^{-1} with a resolution of 4 cm^{-1} (scan number 32). The samples were prepared as suspensions in Nujol between polyethylene windows.

The electrochemical potentials of the studied compounds were measured by cyclic voltammetry (CV) in a three-electrode cell using an IPC-pro potentiostat in CH_2Cl_2 and MeCN under argon. The working electrode was a stationary glassy electrode with a diameter of 2 mm, and a platinum wire ($S = 18$ mm^2) served as an auxiliary electrode. The reference electrode (Ag/AgCl/KCl) had a water-proof membrane. The concentration of the studied compounds was 0.002–0.003 mol/L. The number of electrons transferred during the electrode process was estimated relatively to ferrocene used as a standard. The potential sweep was 0.2 V/s. The supporting electrolyte was 0.1 M Bu_4NClO_4 (99%, Acros) doubly recrystallized from aqueous EtOH and dried in vacuo (48 h) at 50°C.

Synthesis of complexes I–V. Potassium hydroxide (0.071 g, 1.27 mmol) was added to a solution of 2-hydroxy-3,6-di-*tert*-butyl-*p*-benzoquinone (0.3 g, 1.27 mmol) in methanol (20 mL). The reaction mixture was magnetically stirred for 20 min. The color of the solution changed from yellow to violet, indicating the formation of potassium salt LK [16]. The corresponding tin(IV) organochloride (0.635 mmole in the case of Cl_2SnMe_2, Cl_2SnEt_2, $Cl_2Sn(Bu^n)_2$, Cl_2SnPh_2 and 1.27 mmoles for $ClSnMe_3$) was added with stirring to the obtained salt. The formation of compounds **I–V** was accompanied by a change in the solution color from saturated violet to red. The reaction mixture was kept at −18°C for 24 h. Complexes **I–V** were isolated as finely crystalline red powders. All obtained compounds were stable in air in both the solid state and solution.

Complex L_2SnMe_2 (I). The analytically pure product was isolated in an yield of 0.343 g (87%).

For $C_{30}H_{44}O_6Sn$			
anal. calcd., %:	C, 58.17;	H, 7.16;	Sn, 19.17.
Found, %:	C, 58.20;	H, 6.19;	Sn, 19.11.

^1H NMR (400 MHz), δ, ppm: 0.71 (s, 6H, CH_3(Me)), 1.25 (s, 18H, $CH_3(Bu^t)$, where Bu^t = *tert*-butyl), 1.41 (s, 18H, $CH_3(Bu^t)$), 6.35 (s, 2H, $CH_{quinone}$). ^{13}C NMR (100 MHz), δ, ppm: 4.74 (CH_3(Me)), 28.87, 30.22 ($CH_3(Bu^t)$), 34.28, 34.87 ($C(Bu^t)$), 127.99 ($C_{quinone}$–Bu^t), 137.55 ($C_{quinone}$–H), 148.24 ($C_{quinone}$–Bu^t), 158.36 ($C_{quinone}$–O), 188.97, 189.26 ($C_{quinone}$=O). ^{119}Sn NMR (149 MHz), δ, ppm: −152.32.

IR, ν, cm^{-1}: 1619 (C=O), 1554 $(C=C)_{quin.ring}$, $(C–O)_{nonpl}$, 1294 $(C=C)_{quin.ring}$, (C–O), (C–H), 1173 $(C–H)_{Me}$, 1066 (C=C), $(C–H)_{quin.ring}$, 573 $(Sn–C)_{as}$, 521 $(Sn–C)_s$, 542, 484 (Sn–O), 141 (Sn–C).

Complex L_2SnEt_2 (II). The analytically pure product was isolated in an yield of 0.35 g (85%).

For $C_{32}H_{48}O_6Sn$			
anal. calcd., %:	C, 59.36;	H, 7.47;	Sn, 18.34.
Found, %:	C, 59.40;	H, 7.51;	Sn, 18.29.

^1H NMR (400 MHz), δ, ppm: 1.08 (t, $J = 7.88$ Hz, 6H, CH_3(Et)), 1.26 (s, 18H, $CH_3(Bu^t)$), 1.39 (quart., $J = 7.88$ Hz, 4H, CH_2(Et)), 1.41 (s, 18H, $CH_3(Bu^t)$), 6.35 (s, 2H, $CH_{quinone}$). ^{13}C NMR (100 MHz), δ, ppm: 9.1 (CH_3(Et)), 17.84 (CH_2(Et)), 28.89, 30.06 ($CH_3(Bu^t)$), 34.25, 34.80 ($C(Bu^t)$), 127.55 ($C_{quinone}$–Bu^t), 137.69 ($C_{quinone}$–H), 148.08 ($C_{quinone}$–Bu^t), 159.17 ($C_{quinone}$–O), 188.96, 189.59 ($C_{quinone}$=O). ^{119}Sn NMR (149 MHz), δ, ppm: −189.28.

IR, ν, cm^{-1}: 1619 (C=O), 1541 $(C=C)_{quin.ring}$, $(C–O)_{nonpl}$, 1292 $(C=C)_{quin.ring}$, (C–O), (C–H), 1170 $(C–H)_{Et}$, 1066 (C=C), $(C–H)_{quin.ring}$, 522 $(Sn–C)_{as}$, 496 $(Sn–C)_s$, 540, 484 (Sn–O).

Complex $L_2Sn(Bu^n)_2$ (III). The analytically pure product was isolated in an yield of 0.364 g (81.5%).

For $C_{36}H_{56}O_6Sn$			
anal. calcd., %:	C, 61.46;	H, 8.02;	Sn, 16.87.
Found, %:	C, 61.50;	H, 8.05;	Sn, 16.82.

^1H NMR (200 MHz), δ, ppm: 0.81 (t, $J = 7.17$ Hz, 6H, $CH_3(Bu^n)$), 1.27 (s, 18H, $CH_3(Bu^t)$), 1.27–1.41 (m, 12H, $CH_2(Bu^n)$), 1.41 (s, 18H, $CH_3(Bu^t)$), 6.36 (s, 2H, $CH_{quinone}$). ^{13}C NMR (50 MHz), δ, ppm: 13.56 ($CH_3(Bu^n)$), 25.24, 25.99, 26.88 ($CH_2(Bu^n)$), 28.89, 30.16 ($CH_3(Bu^t)$), 34.23, 34.80 ($C(Bu^t)$), 127.69 ($C_{quinone}$–Bu^t), 137.67 ($C_{quinone}$–H), 148.05 ($C_{quinone}$–Bu^t), 158.91 ($C_{quinone}$–O), 189.02, 189.38 ($C_{quinone}$=O). ^{119}Sn NMR (74.6 MHz), δ, ppm: −185.73.

IR, ν, cm^{-1}: 1616 (C=O), 1545 $(C=C)_{quin.ring}$, $(C–O)_{nonpl}$, 1290 $(C=C)_{quin.ring}$, (C–O), (C–H), 1170 $(C–H)_{Bu^n}$, 1070 (C=C), $(C–H)_{quin.ring}$, 515 (Sn–C), 542, 484 (Sn–O).

Complex L_2SnPh_2 (IV). The analytically pure product was isolated in an yield of 0.422 g (89.5%).

For $C_{40}H_{48}O_6Sn$			
anal. calcd., %:	C, 64.62;	H, 6.51;	Sn, 15.97.
Found, %:	C, 64.67;	H, 6.55;	Sn, 15.93.

^1H NMR (400 MHz), δ, ppm: 1.07 (s, 18H, $CH_3(Bu^t)$), 1.48 (s, 18H, $CH_3(Bu^t)$), 6.29 (s, 2H, $CH_{quinone}$), 7.38 (m, 6H, CH(Ph)), 7.65 (m, 4H,

CH(Ph)). ^{13}C NMR (100 MHz), δ, ppm: 28.61, 30.29 ($CH_3(Bu^t)$), 34.19, 35.06 ($C(Bu^t)$), 127.70 ($C_{quinone}$–Bu^t), 128.85, 129.82, 134.86 (C_{Ph}–H), 137.84 ($C_{quinone}$–H), 143.00 (C_{Ph}–Sn), 148.13 ($C_{quinone}$–Bu^t), 157.03 ($C_{quinone}$–O), 188.75, 188.93 ($C_{quinone}$=O). ^{119}Sn NMR (149 MHz), δ, ppm: –113.00 (br).

IR, ν, cm^{-1}: 1619 (C=O), 1592 $(C=C)_{quin.ring}$, 1557 $(C=C)_{quin.ring}$, $(C–O)_{nonpl}$, 1480 $(C=C)_{Ph}$, 1295 $(C=C)_{quin.ring}$, (C–O), (C–H), 1066 (C=C), $(C–H)_{quin.ring}$, 731, 696 $(C=C)_{Ph}$, 550, 480 (Sn–O), 450, 442 $(C=C)_{Ph}$, 273, 245, 229 (Sn–C).

Complex $LSnMe_3$ (V). The analytically pure product was isolated in an yield of 0.395 g (78%).

For $C_{17}H_{28}O_3Sn$			
anal. calcd., %:	C, 51.16;	H, 7.07;	Sn, 29.74.
Found, %:	C, 51.20;	H, 7.11;	Sn, 29.71.

^{1}H NMR (400 MHz), δ, ppm: 0.47 (s, 9H, CH_3(Me)), 1.22 (s, 9H, $CH_3(Bu^t)$), 1.34 (s, 9H, $CH_3(Bu^t)$), 6.29 (s, 1H, $CH_{quinone}$). ^{13}C NMR (100 MHz), δ, ppm: 0.15 (Me), 28.92, 30.48 ($CH_3(Bu^t)$), 34.23, 34.80 ($C(Bu^t)$), 126.45 ($C_{quinone}$–Bu^t), 136.59 ($C_{quinone}$–H), 148.69 ($C_{quinone}$–Bu^t), 156.59 ($C_{quinone}$–O), 186.91, 189.19 ($C_{quinone}$=O). ^{119}Sn NMR (149 MHz), δ, ppm: 126.53.

IR, ν, cm^{-1}: 1660, 1640 (C=O), 1595 $(C=C)_{quin.ring}$, 1535 $(C=C)_{quin.ring}$, $(C–O)_{nonpl}$, 1308 $(C=C)_{quin.ring}$, (C–O), (C–H), 1070 (C=C), $(C–H)_{quin.ring}$, 528 $(Sn–C)_{as}$, 515 $(Sn–C)_s$, 542, 554, 484 (Sn–O), 150 (Sn–C).

Complex $LSnPh_3$ (VI). ^{1}H NMR (400 MHz), δ, ppm: 1.18 (s, 9H, $CH_3(Bu^t)$), 1.43 (s, 9H, $CH_3(Bu^t)$), 6.32 (s, 1H, $CH_{quinone}$), 7.43 (m, 9H, CH(Ph)), 7.77 (m, 6H, CH(Ph)). ^{13}C NMR (100 MHz), δ, ppm: 28.83, 30.41 ($CH_3(Bu^t)$), 34.23, 34.85 $C(Bu^t)$, 127.48 ($C_{quinone}$–Bu^t), 128.68, 129.71, 136.77 (C_{Ph}–H), 137.06 ($C_{quinone}$–H), 141.48 (C_{Ph}–Sn), 148.54 ($C_{quinone}$–Bu^t), 155.60 ($C_{quinone}$–O), 187.08, 188.97 ($C_{quinone}$=O). ^{119}Sn NMR (149 MHz), δ, ppm: –128.68.

IR, ν, cm^{-1}: 1660, 1643 (C=O), 1590 $(C=C)_{quin.ring}$, 1530 $(C=C)_{quin.ring}$, $(C–O)_{nonpl}$, 1480, 1430 $(C=C)_{Ph}$, 1292 $(C=C)_{quin.ring}$, (C–O), (C–H), 1073 (C=C), $(C–H)_{quin.ring}$, 731, 696 $(C=C)_{Ph}$, 535, 483 (Sn–O), 450, 444 $(C=C)_{Ph}$, 282, 261, 235, 221 (Sn–C).

X-ray diffraction analyses of III · MeOH and V. Single crystals suitable for X-ray diffraction analysis were obtained from methanol and diethyl ether, respectively. The X-ray diffraction analysis was carried out on the XCalibur diffractometer (Agilent Technologies, MoK_α, graphite monochromator) at 100(2) K. Structures **III** and **V** were solved by direct methods followed by the refinement using full-matrix least squares for F^2 (SHELXTL) [18]. An absorption correction was applied using the SCALE3 ABSPACK program [19]. All non-hydrogen atoms were refined in the anisotropic approximation. Hydrogen atoms were placed in the geometrically calculated positions and refined in the riding model.

The crystallographic data and the main refinement parameters for structures **III** · MeOH and **V** are listed in Table 1. Selected bond lengths and bond angles are given in Table 2.

The crystallographic data for complexes **III** · MeOH and **V** were deposited with the Cambridge Crystallographic Data Centre (CCDC nos. 947083 (**III** · MeOH) and 947084 (**V**); deposit@ccdc.cam.ac.uk or http://www.ccdc.cam.ac.uk/data_request/cif).

RESULTS AND DISCUSSION

Tin complexes **I–V** are formed in the exchange reaction between potassium salt of 2-hydroxy-*p*-benzoquinone (LK) and the corresponding organotin chlorides in methanol (Scheme 1). The compounds are isolated as finely crystalline red substances in good preparative yields.

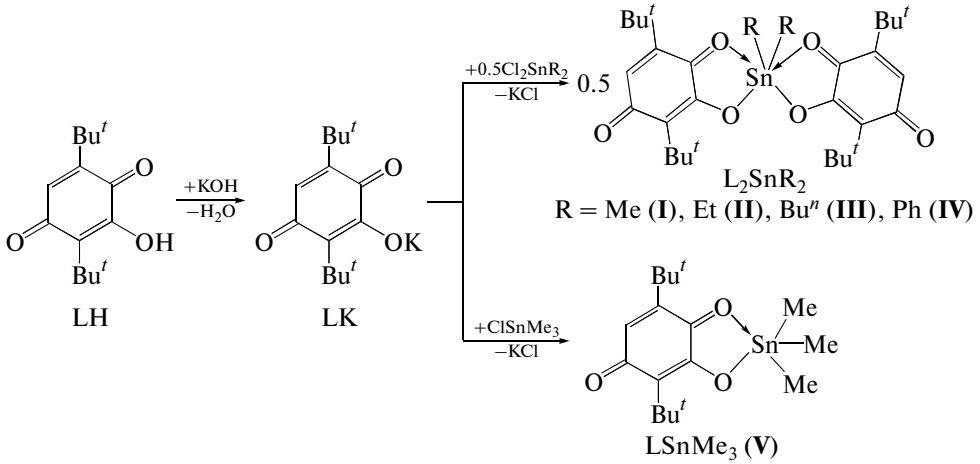

Scheme 1.

Table 1. Crystallographic data and X-ray diffraction experimental and refinement parameters for complexes **III** · MeOH and **V**

Parameter	Value	
	III · MeOH	**V**
Formula	$C_{37}H_{58}O_7Sn$	$C_{17}H_{28}O_3Sn$
Formula weight	733.52	399.08
Crystal system	Triclinic	Monoclinic
Space group	$P\bar{1}$	$P2_1/c$
a, Å	10.50143(15)	16.4327(3)
b, Å	11.0582(2)	6.51409(9)
c, Å	17.3062(2)	18.7340(3)
α, deg	75.5395(15)	90
β, deg	86.7671(12)	112.5085(19)
γ, deg	76.6991(14)	90
V, Å^3	1893.84(5)	1852.60(5)
Z	2	4
F(000)	772	816
ρ_{calcd}, g/cm^3	1.286	1.431
μ, mm^{-1}	0.718	1.386
Crystal size, mm	0.20 × 0.20 × 0.20	0.50 × 0.20 × 0.10
θ Range, deg	3.09–30.00	3.12–26.00
Ranges of reflection indices	$-14 \le h \le 14$, $-15 \le k \le 15$, $-24 \le l \le 24$	$-20 \le h \le 20$, $-8 \le k \le 8$, $-23 \le l \le 23$
Number of independent reflections	37373	26923
Number of observed reflections	10939	3613
R_{int}	0.0531	0.0370
Goodness-of-fit (F^2)	1.004	1.076
R_1, wR_2 ($I > 2\sigma(I)$)	0.0355, 0.0708	0.0256, 0.0626
R_1, wR_2 (for all parameters)	0.0487, 0.0739	0.0291, 0.0642
Residual electron density (max/min), e Å^{-3}	0.852/–0.555	2.431/–0.704

All synthesized complexes **I–V** were characterized by elemental analyses and ^{1}H, ^{13}C, and ^{119}Sn NMR spectroscopy. The molecular structures of complexes **III** · MeOH (hereinafter, **III**) and **V** were determined by X-ray diffraction analysis.

The crystallographic cell of complex **III** contains one solvate methanol molecule per molecule of the complex. The hexacoordinate tin atom in structure **III** is in a strongly distorted octahedral ligand environment (Fig. 1). The O(1), O(2), O(4), and O(5) atoms

of both chelate ligands form a base of the octahedron, and C(29) and C(33) atoms of the *n*-butyl groups are in the apical positions. The value of the C(29)Sn(1)C(33) angle deviates strongly from 180°, being 138.87(14)°. The base of the octahedron is also strongly distorted, and the values of the OSnO angles differ substantially from 90°. The tin atom shifts from the O(1)O(2)O(4)O(5) plane by 0.034 Å. Both chelating monooxy-*p*-benzoquinone ligands are nearly planar, and the dihedral angle between the planes of the ligands is 22.71°. The *n*-butyl groups at the metal atom are in the *cis* position relatively to each other. Ligands L are arranged in such a way that the O(1), O(4) and O(2), O(5) carbonyl atoms are also in pairs in the *cis* position, and the O(1)Sn(1)O(4) and O(2)Sn(1)O(5) angles are 143.16(3)° and 78.17(4)°, respectively. The Sn(1)–O(2) (2.0740(9) Å) and Sn(1)–O(5) (2.0729(10) Å) distances are much shorter than the sum of covalent radii of the Sn and O atoms (2.11 Å [20]), indicating the covalent nature of these bonds. On the contrary, the Sn(1)–O(1) (2.4466(9) Å) and Sn(1)–O(4) (2.4932(9) Å) distances exceed the sum of the covalent radii of the tin and oxygen atoms by more than 0.3 Å but are shorter than the sum of their Van der Waals radii (3.7 Å [20]). Thus, the Sn(1)–O(1) and Sn(1)–O(4) bonds are donor–acceptor. The C(2)–O(2) (1.3139(15) Å) and C(16)–O(5) (1.3143(15) Å) are shorter than typical single carbon–oxygen bonds in the tin(IV) phenolate [21] and catecholate complexes [22, 23] and are closer in values to those characteristic of the tin *o*-semiquinolate derivatives [24, 25]. At the same time, the C(1)–O(1) (1.2257(16) Å) and C(15)–O(4) (1.2308(17) Å) bonds are double. It should be mentioned that the formation of the donor–acceptor interaction between the O(1) and O(4) atoms and the metal center upon complex formation does not elongate the C=O bonds of the ligand. Moreover, these distances do not differ from those of C(4)–O(3) (1.2319(16) Å) and C(18)–O(6) (1.2293(19) Å), although the O(3) and O(6) atoms are not involved in coordination interactions. The *p*-quinoid distribution of double and single bonds is retained in the C(1)–C(6) and C(15)–C(20) six-membered rings. The C(2)–C(3) (1.3666(18) Å) and C(5)–C(6) (1.3315(19) Å) double bonds of one ring and C(16)–C(17) (1.369(2) Å) and C(19)–C(20) (1.341(2) Å) of another ring are separated by two single bonds C(1)–C(2), C(1)–C(6), C(3)–C(4), and C(4)–C(5) (1.4641(17)–1.508(2) Å) in the first ligand and C(15)–C(16), C(15)–C(20), C(17)–C(18), and C(18)–C(19) (1.4776(18)–1.507(2) Å) in the second ligand.

The IR spectroscopic data completely confirm the described structure of compound **III**. The formation of the tin–oxygen covalent bond in the complex is indicated by the presence of absorption bands at 540 and 480 cm^{-1} in the IR spectra characterizing the bending vibrations δ(O–Sn–O) [26–28]. The band at

Table 2. Selected bond lengths (Å) and bond angles (deg) in complexes **III** · MeOH and **V**

Bond	*d*, Å	Bond	*d*, Å
III · MeOH			
Sn(1)–O(1)	2.4466(9)	C(1)–C(2)	1.508(2)
Sn(1)–O(2)	2.0740(9)	C(2)–C(3)	1.3666(18)
Sn(1)–O(4)	2.4932(9)	C(3)–C(4)	1.4641(17)
Sn(1)–O(5)	2.0729(10)	C(4)–C(5)	1.493(2)
Sn(1)–C(29)	2.193(4)	C(5)–C(6)	1.3315(19)
Sn(1)–C(33)	2.142(3)	C(1)–C(6)	1.4842(17)
C(1)–O(1)	1.2257(16)	C(15)–C(16)	1.507(2)
C(2)–O(2)	1.3139(15)	C(16)–C(17)	1.369(2)
C(15)–O(4)	1.2308(17)	C(17)–C(18)	1.4776(18)
C(16)–O(5)	1.3143(15)	C(18)–C(19)	1.483(2)
C(4)–O(3)	1.2319(16)	C(19)–C(20)	1.341(2)
C(18)–O(6)	1.2293(19)	C(15)–C(20)	1.4806(17)
V			
Sn(1)–O(1)	2.754(2)	C(4)–C(5)	1.491(2)
Sn(1)–O(2)	2.1042(12)	C(5)–C(6)	1.331(2)
C(1)–O(1)	1.222(2)	C(1)–C(6)	1.489(2)
C(2)–O(2)	1.304(2)	Sn(1)–C(15)	2.1109(18)
C(4)–O(3)	1.236(2)	Sn(1)–C(16)	2.1331(17)
C(1)–C(2)	1.522(2)	Sn(1)–C(17)	2.1278(16)
C(2)–C(3)	1.378(2)	Sn(1)···O(3')	2.811(2)
C(3)–C(4)	1.465(2)		
Angle	ω, deg	Angle	ω, deg
III · MeOH			
O(5)Sn(1)O(2)	78.17(4)	C(33)Sn(1)O(1)	83.94(8)
O(5)Sn(1)C(33)	102.87(9)	C(29)Sn(1)O(1)	88.48(11)
O(2)Sn(1)C(33)	111.09(9)	O(5)Sn(1)O(4)	68.81(4)
O(5)Sn(1)C(29)	104.84(12)	O(2)Sn(1)O(4)	146.83(4)
O(2)Sn(1)C(29)	103.94(11)	C(33)Sn(1)O(4)	80.27(8)
C(33)Sn(1)C(29)	138.87(14)	C(29)Sn(1)O(4)	82.11(11)
O(5)Sn(1)O(1)	147.69(4)	O(1)Sn(1)O(4)	143.16(3)
O(2)Sn(1)O(1)	70.02(3)		
V			
O(1)Sn(1)C(15)	73.54(7)	O(1)Sn(1)C(16)	154.76(7)
C(15)Sn(1)O(3')	75.53(7)	C(15)Sn(1)C(17)	124.73(7)
O(3')Sn(1)C(17)	84.53(7)	C(15)Sn(1)C(16)	113.61(7)
C(16)Sn(1)C(17)	113.89(7)	O(2)Sn(1)C(15)	103.19(6)
O(2)Sn(1)C(16)	91.03(6)	O(2)Sn(1)O(3')	171.77(7)
O(1)Sn(1)O(2)	63.77(7)	O(3')Sn(1)C(16)	82.19(7)
O(1)Sn(1)O(3')	122.77(7)	O(2)Sn(1)C(17)	102.56(6)
O(1)Sn(1)C(17)	75.57(7)		

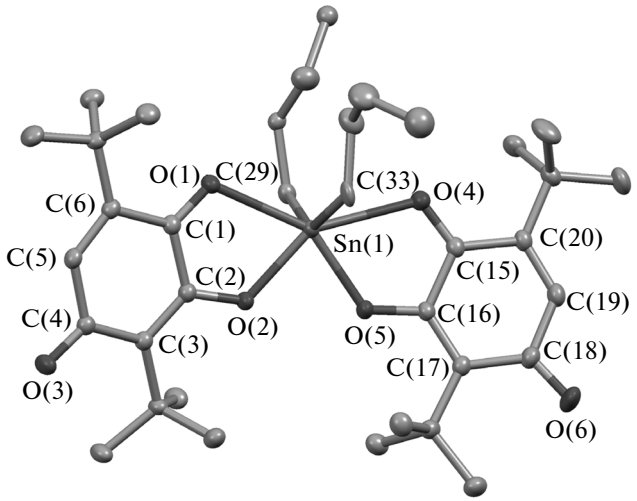

Fig. 1. Molecular structure of complex $L_2Sn(Bu^n)_2$ (**III**). Thermal ellipsoids of 50% probability are presented. Hydrogen atoms are omitted.

~600 cm^{-1} corresponds to mixed stretching vibrations ν(Sn–O), $\nu(C–C)_{quin.ring}$, and ν(C–O) [29–32]. These absorption bands are absent from the IR spectrum of the initial organotin chloride $Cl_2Sn(Bu^n)_2$. The vibrations of the C=O carbonyl groups appear as an intense band at 1616 cm^{-1}. The absorption band at 1545 cm^{-1} characterizes stretching vibrations of the C=C bonds of the quinone rings ν(C=C) [29–32].

The structure of complex **V** (Fig. 2) is similar to that of earlier studied compound $LSnPh_3$ (**VI**) [16].

In crystal, molecules of the complex are bound into polymer one-dimensional chains of the coordination polymer by a donor–acceptor bond between the metal center and O(3) atom of the adjacent molecule. As in compounds **III** and **VI**, the tin atom in complex **V** has a distorted octahedral environment by the O(1) and O(2) atoms of one monooxy-*p*-quinone ligand, the O(3) atom of the adjacent molecule, and three carbon atoms of the methyl groups. The base of the octahedron is formed by three oxygen atoms and the C(16) atom of one of the methyl substituents, and the C(15) and C(17) atoms occupy the apical positions. The Sn(1) atom shifts from the O(1)O(2)O(3)C(16) plane by 0.08 Å. The C(15)Sn(1)C(17) angle is 124.73(7)°, which is also considerably smaller than a value of 180° characteristic of an octahedron. The Sn(1)–O(2) bond (2.1042(12) Å) is covalent, whereas the Sn(1)–O(1) (2.754(2) Å) and Sn(1)–O(3) (2.811(2) Å) distances significantly exceed the sum of the covalent radii of the corresponding Sn and O atoms (2.11 Å [20]), indicating their donor–acceptor nature. In complex **V** these bonds are considerably longer than the corresponding bonds in compound **III** and, as a consequence, should be weaker. As in compound **III**, in compound **V** the C(2)–O(2) bond (1.304(2) Å) is shorter than the typical single carbon–oxygen bond and the C(1)–O(1) (1.222(2) Å) and C(4)–O(3) (1.236(2) Å) distances are characteristic of double bonds. It should be mentioned that, as in compounds **III** and **VI**, in **V** the coordination of the O(1) and O(3) atoms with the metal center does not elongate the C=O bonds. The double and single C–C bonds alternate in the six-membered carbon cycle of the monooxy-*p*-quinone ligand. The C(2)–C(3) (1.378(2) Å) and C(5)–C(6) (1.331(2) Å) bonds are separated by two single bonds C(1)–C(2), C(1)–C(6), C(3)–C(4), and C(4)–C(5) (1.465(2)–1.522(2) Å).

As mentioned above, the Sn(1)–O(3) bond in compound **V** is fairly long (2.811(2) Å) and comparable with the corresponding bond in complex **VI** (2.821(5) Å) [16]. As reported in [16] devoted to the study of the structure of compound **VI**, the structure of the coordination polymer existing in crystal is decomposed in solution because of the cleavage of the tin–oxygen donor–acceptor bonds in the adjacent molecule. In a solution of $LSnMe_3$, most likely, the Sn(1)–O(3) bonds are also decomposed, which is indicated by the value of the chemical shift of the signal in the ^{119}Sn NMR spectrum. Unlike compounds **I–IV** and **VI**, only complex **V** is characterized by the positive chemical shift in this spectrum, which is a consequence of a decrease in the coordination number of the metal atom [33].

According to the comparative analysis of the IR spectra of compounds **V** and **VI** in the long-wavelength region, a frequency of ~600 cm^{-1} corresponds to vibrations of the tin–oxygen bond. As already men-

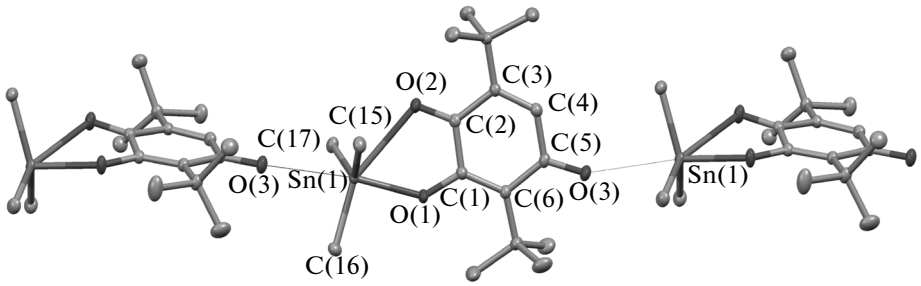

Fig. 2. Fragment of the crystal packing of complex $LSnMe_3$ (**V**). Thermal ellipsoids of 50% probability are presented. Hydrogen atoms are omitted.

Table 3. Electrochemical potentials of complexes **I**–**VI** and LH according to the CV data*

Compound	$E_{1/2}^{Red.1}$, V	n	I_a/I_c	$E_{1/2}^{Red.2}$, V	n	I_a/I_c	$E^{Ox.1}$, V	$E^{Ox.2}$, V
LH	–0.57[a]	1		–1.44	1	0.6	1.96[c]	
I	–0.40	1	0.8	–1.45	2	0.7	1.80	
II	–0.47	1	0.9	–1.43	2	0.9	1.66	1.78
III	–0.47	1	0.7	–1.43	2	0.7	1.65	1.80
IV	–0.29	1	1.0	–0.74	$n < 1$	1.0	1.80[b]	
V	–0.56	1	0.6	–1.44	1	0.7	1.51	1.71
VI	–0.47	1	0.9	–1.44	1	0.6	1.82[b]	

* Glassy carbon electrode, CH_2Cl_2, $V = 0.2$ V/s, vs. Ag/AgCl/KCl, $c = 3 \times 10^{-3}$ mol/L, Ar, 0.1 M Bu_4NClO_4; $E_{1/2}^{Red.1}$ is the potential of the half-wave of the first cathodic process, $E_{1/2}^{Red.2}$ is the potential of the half-wave of the second cathodic process, E^{Ox} is the potential of the oxidation peak, I_a/I_c is the ratio of currents of the inverse cathodic and direct anodic peaks, and n is the number of electrons transferred in the course of the redox process relatively to ferrocene used as a standard; [a] is the potential of the reduction peak for the irreversible process, [b] is the irreversible two-electron process, and [c] the data obtained in MeCN.

tioned, the same region contains the bands corresponding to bending vibrations of the C–C bonds of the quinone rings. Therefore, this band is broadened in the spectra of compounds **V** and **VI**. In the spectra of solutions of the compounds in CCl_4, the band at 609 cm^{-1} corresponds to these vibrations. In the spectra of the polycrystalline samples, this band is split into two components: at 600 and 615 cm^{-1}. In the IR spectrum of complex $LSnMe_3$, the bands at 554 and 541 cm^{-1} correspond to the δ(O–Sn–O) vibrations. In the spectra of a solution in CCl_4, the corresponding absorption bands are observed in a lower-frequency range: at 543 and 534 cm^{-1}. In compound $LSnPh_3$, this type of vibrations has the absorption band at 535 cm^{-1}, which is shifted to 544 cm^{-1} in the spectrum of a solution in CCl_4. The absorption bands at 1660 and 1640 cm^{-1} are due to stretching vibrations of the carbonyl groups of the ligand, whereas two intense bands at 1530 and 1595 cm^{-1} characterize vibrations of the carbon–carbon bonds of the quinone rings.

The study of the far range of the IR spectra (600–150 cm^{-1}) makes it possible to identify the tin–oxygen and tin–carbon bonds in complexes **I–VI**.

Based on the comparative analysis of the experimental spectra of compounds **I–III** and **V** and the starting organotin chlorides and taking into account the published data, it was established that the absorption bands at 573 and 521 cm^{-1} (**I**) [26, 34–36], 522 and 496 cm^{-1} (**II**) [34–36], 515 cm^{-1} (**III**) [26, 34–36], and 528 and 515 cm^{-1} (**V**) [35] were assigned to asymmetric and symmetric vibrations of the tin–carbon bonds. In the IR spectra of complex L_2SnMe_2 and the starting chloride Cl_2SnMe_2, the absorption band at 143 cm^{-1} corresponds to the bending vibrations δ(C–Sn–C).

According to published data [37, 38], the tin–carbon bond vibrations of the phenyl rings should correspond to the absorption bands at 460–440, 250–230, 230–195, and 185–160 cm^{-1}. A comparison of the IR spectra of compounds **IV** and **VI** and the starting diphenyltin(IV) dichloride Cl_2SnPh_2 showed that the absorption bands at 230 and 245 cm^{-1} for L_2SnPh_2 and a group of bands at 260, 235, 222, and 214 cm^{-1} for $LSnPh_3$ correspond to the bending wagging and scissoring vibrations δ(C–Sn–C). The absorption bands at 280 (**IV**) and 283 cm^{-1} (**VI**) characterize the stretching vibrations ν(Sn–C) [26, 34, 37, 38]. The doublet with peaks at 450 and 442 cm^{-1} retaining its position in the initial organotin chloride and in complexes **IV** and **VI** is caused by the vibrations of the tin–carbon bond of the phenyl rings.

The electrochemical transformations of tin complexes **I–VI** and LH were studied by CV. The values of redox potentials of the studied compounds are given in Table 3. Unlike the classical two-stage scheme for *p*-benzoquinone reduction [39] including two reversible one-electron processes, the electrochemical reduction of 2-hydroxy-*p*-quinones is accompanied by self-protonation reactions caused by the high acidity of the hydroxy group [40].

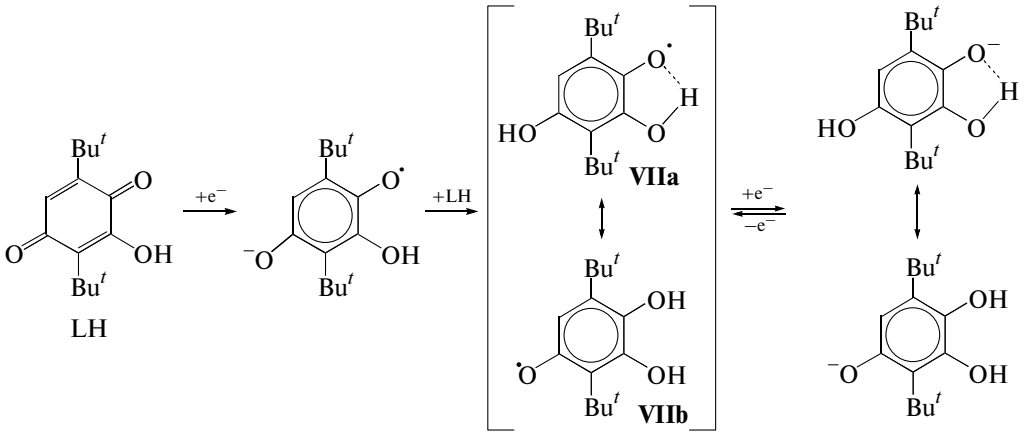

Scheme 2.

The irreversible one-electron process is observed at the first stage of the electrochemical reduction of LH. The electron transfer is followed by the fast chemical stage, being the protonation of the radical anion formed in the electrochemical reaction by the adjacent *p*-quinone molecule to form phenoxyl radical **VII** (Scheme 2). The latter can be presented by two tautomeric forms **VIIa** and **VIIb**. Intermediate **VIIa** is stabilized by the interaction with the hydrogen atom of the adjacent hydroxy group. The second cathodic process is one-electron and quasi-reversible. Evidently, the phenoxyl radical formed in the chemical reaction is reduced to the corresponding anion.

No electrochemical activity of this *p*-benzoquinone is detected in dichloromethane in the anodic region (below 1.80 V) in the considered potential scan range. The oxidation peak at the high anodic potential (1.96 V) was detected in acetonitrile.

Monoligand complexes **V** and **VI** in dichloromethane are electrochemically reduced in two successive quasi-reversible one-electron stages (Fig. 3) accompanied by a change in the oxidation state of the coordinated redox-active ligand. As a result of the electron transfer, the corresponding mono- and dianionic complexes are generated in the near-electrode zone (Scheme 3).

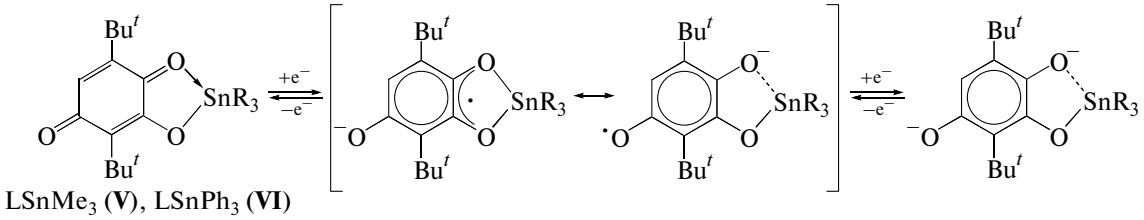

Scheme 3.

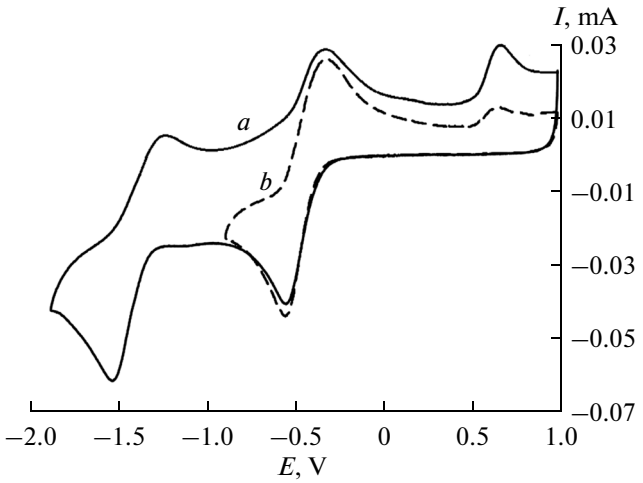

Fig. 3. Cyclic voltammogram of the reduction of complex **VI** in the potential scan ranges (a) from 1.0 to −2.0 V and (b) from 1.0 to −0.9 V; glassy carbon anode, Ag/AgCl/KCl, 0.1 M NBu_4ClO_4, argon (the same in Figs. 4 and 5); $c = 3 \times 10^{-3}$ mol/L.

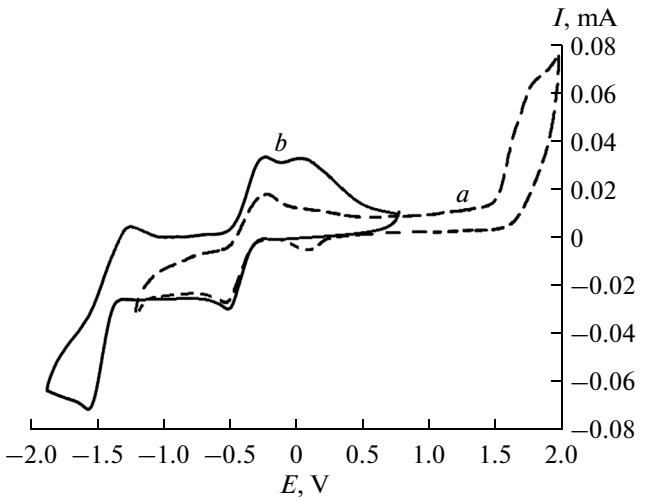

Fig. 4. Cyclic voltammogram for complex **I** in the potential scan ranges (a) from −1.2 to 2.0 V and (b) from 0.79 to −1.87 V; $c = 2 \times 10^{-3}$ mol/L.

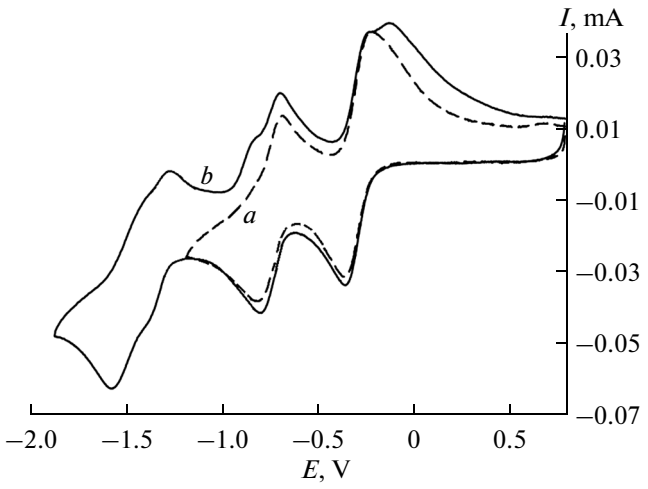

Fig. 5. Cyclic voltammogram for complex **IV** in the potential scan ranges (a) from 0.8 to −1.2 V and (b) from 0.8 to −1.9 V; $c = 2 \times 10^{-3}$ mol/L.

Unlike free *p*-benzoquinone, the first redox transition for complexes **V** and **VI** becomes quasi-reversible due to the absence of proton donors in the medium. The coordination of the ligand to the tin atom favors the stabilization of the reduced forms of the complexes (Table 3). Based on the reversibility coefficient (I_a/I_c), we can conclude that the stability of the monoanionic forms of the complexes depends on the nature of the organic group at the metal atom. For compound **V**, the coordination of the redox-active ligand with the trimethylstannyl group exerts almost no effect on the reduction potential. The replacement of the organic substituents at the metal atom by the phenyl substituents in complex **VI** results in the anodic shift of the reduction potential by 0.1 V and enhances the stability of the reduced form. Taking into account the shift of the first reduction potential depending on the organic substituent at the metal atom, it can be assumed that an electron in the formed semiquinone radical is partially localized in the metallocycle, and a portion of the electron density is also localized on the O(3) oxygen atom (Scheme 3).

For the potential scan below −2.0 V, the second quasi-reversible redox transition accompanied by the chemical stage in solution is detected, and an increase in the peak current of the reaction product (0.65 V) is observed on the inverse branch of the voltammogram. The detected reduction potentials ($E_{1/2}^{Red.2}$) for compounds **V** and **VI** and the starting monohydroxy-*p*-quinone are identical, and no influence of the tin atom and organic moieties is observed.

The electrochemical behavior of compounds **V** and **VI** is different in the anodic region: complex $LSnPh_3$ is oxidized in one irreversible two-electron stage. In the case of $LSnMe_3$, two consecutive oxidation stages shifted to the cathodic region are observed. The nature of the organic group at the tin atom also affects the oxidation of complexes **V** and **VI**: the donor methyl groups facilitate the oxidation process.

The electrochemical reduction of bis(ligand) tin complexes **I–III** proceeds in two quasi-reversible stages (Fig. 4) corresponding to a change in the redox state of the coordinated ligand (Scheme 4).

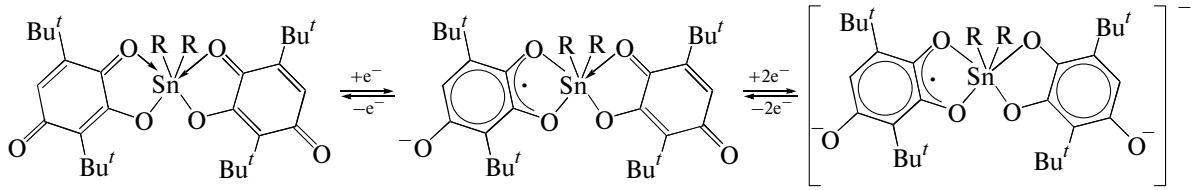

L_2SnMe_2 (**I**), L_2SnEt_2 (**II**), $L_2SnBu_2^n$ (**III**)

Scheme 4.

The first redox transition corresponds to the transfer of one electron, and the second transition is two-electron. The nature of the hydrocarbon fragments at the tin atom affects the value of the potential of the first cathodic stage. The replacement of the methyl group by ethyl one impedes the reduction process.

However, this effect decays already in the case of complex **III**. The obtained electrochemical data presented in Table 3 (I_a/I_c) show that monoanionic complex **II** has the highest stability. For complexes **I–III**, the second cathodic process is characterized by the transfer of two electrons at the potential value close to the second reduction potential of the starting LH. The peak (0.06 V) of the product of the partial decomposition of the reduced complex, which is formed due to the decoordination of one of the ligands, appears on the inverse CV branch at the potential scan below –1.87 V.

The electrochemical oxidation of complexes **I–III** is irreversible and results in their destruction. For compounds **II** and **III**, two anodic stages are observed. The first of them is one-electron. One two-electron stage is detected for the oxidation of complex **I** (Fig. 4).

The electrochemical behavior of L_2SnPh_2 (**IV**) differs from those of compounds **I–III** (Fig. 5). Four quasi-reversible redox transitions are observed for this complex. The general scheme of redox transformations of complex **IV** (Scheme 5) ignoring the chemical processes that occur at the third and fourth stages can be presented as follows:

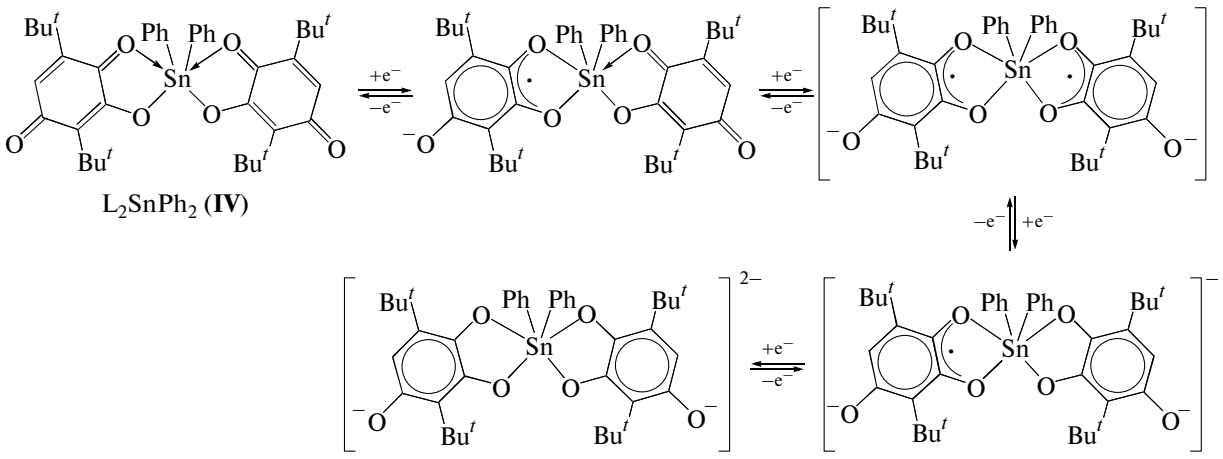

L_2SnPh_2 (**IV**)

Scheme 5.

The parameter ($E_{1/2}^{Red.1}$) for the first reversible one-electron process is substantially shifted to the anodic region compared to the similar value for compounds **I–III**. The second redox transition is also reversible, but the number of electrons transferred in the course of the electrodic process is lower than unity. A significant shift to the positive region of the first and second reduction potentials of complex **IV** compared to those of the free ligands and compound **VI** indicates an increase in the oxidation ability of the redox-active ligand upon the coordination of the carbonyl oxygen atom to the metal atom.

The quasi-reversible third ($E^{Red.3} = -1.38$ V) and fourth ($E^{Red.4} = -1.57$ V) redox processes corresponding to the further reduction of the ligands are observed for the potential scan below –1.90 V (Fig. 5*b*). The completely reduced forms of complex **IV** undergo fast transformations in solution, due to which the oxidation peaks of the chemical reaction products are observed on the inverse CV branch. As in the case of complex $LSnPh_3$, the acceptor phenyl groups favor the stabilization of the reduced mono- and dianionic forms of the complex (Table 3). The third and fourth stages are partially reversible and the reduction potentials are less separated ($\Delta E = 0.19$ V), indicating a low degree of repulsion of the charges and the spatial remoteness of two redox centers.

The electrochemical oxidation of complex **IV** proceeds as one irreversible two-electron stage at a potential close to that of monoligand compound **VI** and is accompanied by the destruction of the complex.

ACKNOWLEDGMENTS

This work was supported by the Russian Foundation for Basic Research (project no. 14-03-31069-mol_a) and the Council on Grants at the President of the Russian Federation for support of leading scientific schools (NSh-271.2014.3).

REFERENCES

1. Abakumov, G.A., Poddel'sky, A.I., Grunova, E.V., et al., *Angew. Chem., Int. Ed. Engl.*, 2005, vol. 44, no. 18, p. 2767.
2. Cherkasov, V.K., Abakumov, G.A., Grunova, E.V., et al., *Chem.-Eur. J.,* 2006, vol. 12, no. 14, p. 3916.
3. Poddel'sky, A.I., Kuskii, Y.A., Piskunov, A.V., et al., *Appl. Organomet. Chem.*, 2011, vol. 25, no. 3, p. 180.
4. Fukin, G.K., Baranov, E.V., Jelsch, C., et al., *J. Phys. Chem., A*, 2011, vol. 115, no. 29, p. 8271.

5. Fukin, G.K., Baranov, E.V., Poddel'sky, A.I., et al., *Chem. Phys. Chem.*, 2012, vol. 13, no. 17, p. 3773.
6. Ilyakina, E.V., Poddel'sky, A.I., Cherkasov, V.K., and Abakumov, G.A., *Mendeleev Commun.*, 2012, vol. 22, no. 4, p. 208.
7. Fedushkin, I.L., Nikipelov, A.S., and Lyssenko, K.A., *J. Am. Chem. Soc.*, 2010, vol. 132, no. 23, p. 7874.
8. Fedushkin, I.L., Nikipelov, A.S., Morozov, A.G., et al., *Chem.-Eur. J.*, 2012, vol. 18, no. 1, p. 255.
9. Fedushkin, I.L., Moskalev, M.V., Lukoyanov, A.N., et al., *Chem.-Eur. J.*, 2012, vol. 18, no. 36, p. 11264.
10. Piskunov, A.V., Meshcheryakova, I.N., Fukin, G.K., et al., *Dalton Trans.*, 2013, vol. 42, no. 29, p. 10533.
11. Abakumov, G.A., Cherkasov, V.K., Piskunov, A.V., et al., *Dokl. Ross. Akad. Nauk*, 2009, vol. 427, no. 3, p. 330.
12. Piskunov, A.V., Mescheryakova, I.N., Bogomyakov, A.S., et al., *Inorg. Chem. Commun.*, 2009, vol. 12, no. 10, p. 1067.
13. Valla, V., Bakola-Christianopoulou, M., Akrivos, P., et al., *Synth. React. Inorg. Met.-Org. Chem.*, 2006, vol. 36, no. 10, p. 765.
14. Valla, V., Bakola-Christianopoulou, M., Kojic, V., and Bogdanovic, G., *Synth. React. Inorg. Met.-Org. Chem.*, vol. 37, no. 1, p. 41.
15. Valla, V. and Bakola-Christianopoulou, M., *Synth. React. Inorg. Met.-Org. Chem.*, 2007, vol. 37, no. 7, p. 507.
16. Kabarova, N.Yu., Cherkasov, V.K., Zakharov, L.N., et al., *Izv. Ross. Akad. Nauk, Ser. Khim.*, 1992, no. 12, p. 2798.
17. Kocheshkov, K.A., in *Metody elementoorganicheskoi khimii. Germanii, olovo, svinets* (Methods of Organoelement Chemistry. Germanium, Tin, Lead), Moscow: Nauka, 1968, p. 704.
18. Sheldrick, G.M., *SHELXTL Version 6.12. Structure Determination Software Suite*, Madison (WI, USA): Bruker AXS, 2000.
19. *SCALE3 ABSPACK. Empirical Absorption Correction Using Spherical Harmonics CrysAlis Pro*, Yarnton (England): Agilent Technologies Ltd., 2011.
20. Batsanov, S.S., *Zh. Neorg. Khim.*, 1991, vol. 36, no. 12, p. 3015.
21. Jurkschat, K., Pieper, N., Seemeyer, S., et al., *Organometallics*, 2001, vol. 20, no. 5, p. 868.
22. Lado, A.V., Piskunov, A.V., Cherkasov, V.K., et al., *Rus. J. Coord. Chem.*, 2006, vol. 32, no. 3, p. 173.
23. Piskunov, A.V., Lado, A.V., Fukin, G.K., et al., *Heteroatom. Chem.*, 2006, vol. 17, no. 6, p. 481.
24. Ilyakina, E.V., Poddel'sky, A.I., Piskunov, A.V., et al., *Inorg. Chim. Acta*, 2012, vol. 380, no. 1, p. 57.
25. Ilyakina, E.V., Poddel'sky, A.I., Piskunov, A.V., et al., *Inorg. Chim. Acta*, 2013, vol. 394, no. 1, p. 282.
26. Pettinari, C., Marchetti, F., Pettinari, R., et al., *Inorg. Chim. Acta*, 2001, vol. 325, nos. 1–2, p. 103.
27. Morrison, J.S. and Haendler, H.M., *J. Inorg. Nucl. Chem.*, 1967, vol. 29, p. 393.
28. Kolb, U. and Drager, M., *Spectrochim. Acta, Part A*, 1997, vol. 53, no. 4, p. 517.
29. Liu, R., Zhou, X., and Pulay, P., *J. Phys. Chem.*, 1992, vol. 96, no. 11, p. 4255.
30. Merienne-Lafore, M.F., *Spectrochim. Acta, Part A*, 1976, vol. 32, no. 5, p. 1235.
31. Dunn, T.M. and Francis, A.H., *J. Mol. Spectrosc.*, 1974, vol. 50, nos. 1–3, p. 1.
32. Nonella, M. and Brandli, C., *J. Phys. Chem.*, 1996, vol. 100, no. 34, p. 14549.
33. Wrackmeyer, B., *Annu. Rep. NMR Spectrosc.*, 1985, vol. 16, p. 73.
34. Alvarez-Boo, P., Casas, J.S., Castineiras, A., et al., *Inorg. Chim. Acta*, 2003, vol. 353, no. 1, p. 8.
35. Dernova, V.S. and Kovalev, I.F., in *Kolebatel'nye spektry soedinenii elementov IVB gruppy* (Vibrational Spectra of Compounds of Group IVB Elements), Sarat. Univ., 1979, p. 300.
36. Chumaevskii, N.A., in *Kolebatel'nye spektry elementoorganicheskikh soedinenii elementov IVB i VB grupp* (Vibrational Spectra of Organoelement Compounds of Group IVB and VB Elements), Moscow: Nauka, 1971, p. 244.
37. Bishop, M.E., Schaeffer, C.D., Jr., Zuckerman, J.J., et al., *Spectrochim. Acta, A*, 1976, vol. 32, no. 8, p. 1519.
38. Poller, R.C., *J. Inorg. Nucl. Chem.*, 1962, vol. 24, no. 5, p. 539.
39. *The Chemistry of the Quinonoid Compounds*, Patai, S. and Rappoport, Z., Eds., New York: Wiley, 1974, vol. 1, p. 737.
40. Costentin, C., *Chem. Rev.*, 2008, vol. 108, no. 7, p. 2145.

Translated by E. Yablonskaya